

Surgically Induced Focal Retinal Detachment Does Not Cause Detectable SD-OCT Retinal Changes in Normal Human Retina

Kaitlin Kogachi,¹ Jeremy D. Wolfe,² and Amir H. Kashani¹

¹USC Roski Eye Institute, Keck School of Medicine of USC, Los Angeles, California, United States

²Associated Retinal Consultants, Oakland University William Beaumont School of Medicine, Royal Oak, Michigan, United States

Correspondence: Amir H. Kashani, USC Roski Eye Institute, Keck School of Medicine of USC, 1450 San Pablo Street, Suite 4700, Los Angeles, CA 90033, USA; ahkashan@usc.edu.

Submitted: August 1, 2017

Accepted: September 18, 2017

Citation: Kogachi K, Wolfe JD, Kashani AH. Surgically induced focal retinal detachment does not cause detectable SD-OCT retinal changes in normal human retina. *Invest Ophthalmol Vis Sci.* 2017;58:5270–5279. DOI: 10.1167/iovs.17-22737

PURPOSE. Induction of focal retinal detachment (RD) for subretinal delivery of stem cells and gene therapy is increasingly common. In order to determine if this procedure has an adverse impact on the retina, we use spectral-domain optical coherence tomography (SD-OCT) to evaluate the pre- and postoperative retinal anatomy of the incidentally detached normal retina surrounding large submacular hemorrhages (SMH) during surgical displacement procedures.

METHODS. Retrospective, observational study of human subjects with monocular SMH evaluated before and after surgical displacement using clinical exam, fundus photography, and SD-OCT. Manual measurements of the inner retinal thickness (IRT), outer retinal thickness (ORT), and full retinal thickness (FRT) were made in regions involving the SMH and surrounding normal retina. Comparison of retinal thickness measurements was made using the Wilcoxon signed-rank test.

RESULTS. Seven eyes were included in this study. All eyes successfully underwent surgical displacement of SMH. Visual acuity improved in 6/7 subjects and was unchanged in the remaining subject. Incidental RD of the normal retinal regions surrounding the SMH did not cause any significant change in IRT, ORT, or FRT that was detectable by SD-OCT. In contrast, mean FRT overlying regions with SMH was significantly greater before surgery compared to after displacement of SMH or normal adjacent retina.

CONCLUSIONS. Surgically induced focal RD does not cause detectable retinal changes in the incidentally detached normal retina surrounding large SMH. Therefore, surgical induction of focal RD should not be considered to have the same adverse impact on the retina as pathologic RD.

Keywords: retinal detachment, submacular hemorrhage, optical coherence tomography, subretinal tissue plasminogen activator

A growing body of literature suggests that gene therapy and stem cell–based therapies of the retina and RPE are possible and even efficacious. Induction of focal retinal detachment (RD) is necessary for the subretinal delivery of these therapies,^{1,2} and a large body of literature has demonstrated that photoreceptors die when separated from the RPE.³ It is not known if surgically induced RD has the same adverse consequences for the retina as pathologic RD or other animal models of RD. Therefore, it is necessary to understand the impact of a focally induced surgical RD on the living human retina to maximize the success of the surgeries that use this technique and minimize the damage to the neurosensory retina and RPE.

Several animal studies have demonstrated that induction of RD causes damage to the overlying neurosensory retina.⁴ For example, induction of RD in rabbits using physiologic solution (balanced salt solution or its equivalent) causes almost immediate microscopic intracellular and extracellular edema throughout the retina and RPE based on histologic studies performed on enucleated eyes immediately following the surgical procedure.^{5,6} It is questionable whether these effects are long-term changes lasting for months to years. These studies

have also indicated that perfusing the vitreous with a modified solution prior to artificial RD can reduce the adhesiveness of the retina to the RPE and decrease the ultrastructural damage.^{5,6} Another study indicated induction of chronic RD in mice with sodium hyaluronate causes photoreceptor apoptosis, focal inflammatory response within the inner retina, and loss of photoreceptors at 24 hours with subsequent progressive loss over several days.⁷ In these mice, histology demonstrates 10% to 15% decrease in outer nuclear layer (ONL) thickness over 7 days.⁷ Similar findings have been demonstrated in the cat⁸ and rat⁹ using sodium hyaluronate to cause chronic RD. The presence of photoreceptor apoptosis in human subjects with naturally occurring, pathologic rhegmatogenous RD (RRD) of at least 1-day duration has also been demonstrated, suggesting that a similar mechanism of retinal damage occurs in human subjects.¹⁰

Although animal and histologic studies are useful, in vivo evaluation of the retina using spectral domain–optical coherence tomography (SD-OCT) has provided a wealth of knowledge regarding pathologic changes associated with RRD in humans.^{11–13} Gharbiya et al.¹¹ demonstrated defects in the external limiting membrane (ELM), ellipsoid zone (EZ), and

cone outer segment tips in up to 52% of patients with macula-off RRD up to several months after successful RD repair. These findings were significantly correlated with postoperative visual outcomes. There was a significant difference in visual outcome between subjects with greater than 200 μm of outer retinal pathology and those with less than 200 μm . In addition, subjects with macula-off RRD had significant thinning of the ONL compared with fellow control eyes. Dell’Omo et al.¹³ conducted a prospective, observational study of foveal structure after RRD repair using serial SD-OCT scans and automatic image registration to ensure the same location was scanned repeatedly over the course of 12 months. This study showed that the retinal layers and the retina overall were thinner 1 month after RRD repair compared with the contralateral, control eye. However, there was gradual increase in retinal thickness and improvement in visual acuity over the subsequent 12 months.¹³ These studies clearly suggest that SD-OCT can detect subclinical, but visually significant, pathologic changes in the retina after RRD and corroborate animal and histologic studies that demonstrate retinal damage.

In contrast to these studies, there is a growing body of literature that suggests focal surgical induction of RD, also called “blebs,” for delivery of gene or stem cell–based therapy does not cause long-term harm and may actually improve vision in pathologic conditions.^{1,2,14,15} Unlike pathologic RRD and experimentally induced chronic RD in animal models, surgically induced RD in human subjects lasts less than 24 hours (and likely less than several hours). This is because only a focal RD is induced during human surgery using balanced salt solution that is easily evacuated by the RPE. However, it is not known if this induced form of focal and short-duration RD causes damage to the retina. It was the goal of our current study to find a way to determine whether surgically induced focal RD has any measurable impact on the retinal anatomy of human subjects.

Human patients with a large submacular hemorrhage (SMH) often undergo pars plana vitrectomy (PPV) with induction of a focal RD for displacement of the SMH.^{16–22} Although this is not a universal practice, many studies have demonstrated at least some efficacy of this method.^{16–18,20,21} Successful surgical displacement of a SMH requires a focal RD (bleb) that necessarily extends outside the region of the SMH. Therefore, a small region of normal, nondetached retina outside the region of SMH is necessarily detached to achieve the goals of the surgery. In this retrospective study, we aimed to determine whether the incidental induction of a RD in the region surrounding the SMH caused any changes in the normal retinal structure of that region using SD-OCT. This is the first and only study that we are aware to examine the impact of surgically induced, focal RD on normal human macular anatomy and provides valuable data for gene therapy and cell-based studies of retinal disease.

MATERIALS AND METHODS

Patients

This was a two-site, observational, retrospective study of human subjects approved by the USC Institutional Review Board (IRB), as well as the Western IRB for the respective sites involved. The methods were in compliance with the criteria described by the Declaration of Helsinki. The study consisted of a retrospective chart review of subjects with a history of SMH and subsequent medically indicated therapeutic intervention including PPV and subretinal displacement of SMH using tissue plasminogen activator (tPA). Subjects with SMH were included if the following criteria were met: (1) occurrence of a

large SMH treated with PPV and subretinal tPA displacement, (2) high-quality OCT scans captured on a Heidelberg Spectralis SD-OCT device (Heidelberg Engineering, Inc., Franklin, MA, USA) of pathologic and normal retinal areas on one occasion prior to surgery and another following surgery, and (3) resolution of the SMH as determined by the color images and OCT scans. The last criterion was necessary to ensure that accurate measurements of the retina could be made without potential confounding effects of subretinal heme on OCT measurements. Patients with poor-quality images or lack of sufficient images to document the extent of the SMH and surgical detachment were excluded. All surgeries were performed by one of two surgeons (JDW or AHK), and the extent of RD induced in the cases was known to be at least one disc diameter outside the region of SMH.

PPV and Subretinal tPA Injection

Surgical procedures were performed using standard 23- or 25-gauge PPV methods on a Constellation (Alcon, Inc., Ft. Worth, TX, USA) vitrectomy system and standard cannula placement 3.5 mm posterior to the limbus. Balanced salt solution (BSS-Plus; Alcon, Inc.) was used for irrigation of the eye during vitrectomy. Intraocular visualization was achieved using the OPMI Lumera 700 surgical microscope with ReSight viewing system (Carl Zeiss Meditec, Inc., Dublin, CA, USA) or a similar system. A posterior vitreous detachment was induced if not already present in all cases. A 41-gauge subretinal infusion cannula (MedOne Surgical, Inc., Sarasota, FL, USA) was used to induce the focal RD starting in the inferior or superior edge of the SMH. In all cases, the procedure included a subretinal injection of tPA (25–50 $\mu\text{g}/0.1\text{ mL}$) sufficient to detach the complete area of the SMH, as well as at least one disc diameter of normal retina in all directions surrounding the SMH. In most cases, the detachment extended more peripherally, and the detachment was confirmed intraoperatively by the surgeon without the use of a hand-held OCT. A 50% to 75% air fill was performed in all subjects to aid in displacement of SMH. In all cases, the area of induced RD was completely reattached on clinical examination postoperative day 1. Subjects were seen for postoperative follow-up at 1 day, 1 week, and 1 month, and subsequently, at the discretion of the surgeon and based on medical need. No subjects required additional procedures and no recurrence of hemorrhage was noted.

Chart Review

The following patient demographics and clinical data were collected from subject medical records: age, sex, preoperative best-corrected visual acuity (BCVA), final postoperative BCVA at the latest follow-up, preoperative IOP, final postoperative IOP at the latest follow-up, and clinical characteristics of the SMH prior to surgery and following surgery. BCVA was recorded as Snellen visual acuity or count fingers (CF), hand motion (HM), or light perception (LP) and converted to logarithm of the minimum angle of resolution (logMAR) for statistical analysis. Visual acuity classified as LP, HM, and CF were converted to logMAR equivalents of 3.0, 2.3, and 1.9, respectively, according to a previously published report.²³ Fundus photographs of the pre- and postoperative affected eye were also obtained for visualization of the SMH and its anatomic borders.

SD-OCT Retinal Image Analysis

SD-OCT images were manually analyzed with the caliper feature on the Heidelberg Spectralis commercial software by one of the authors (KK) and validated by the senior author

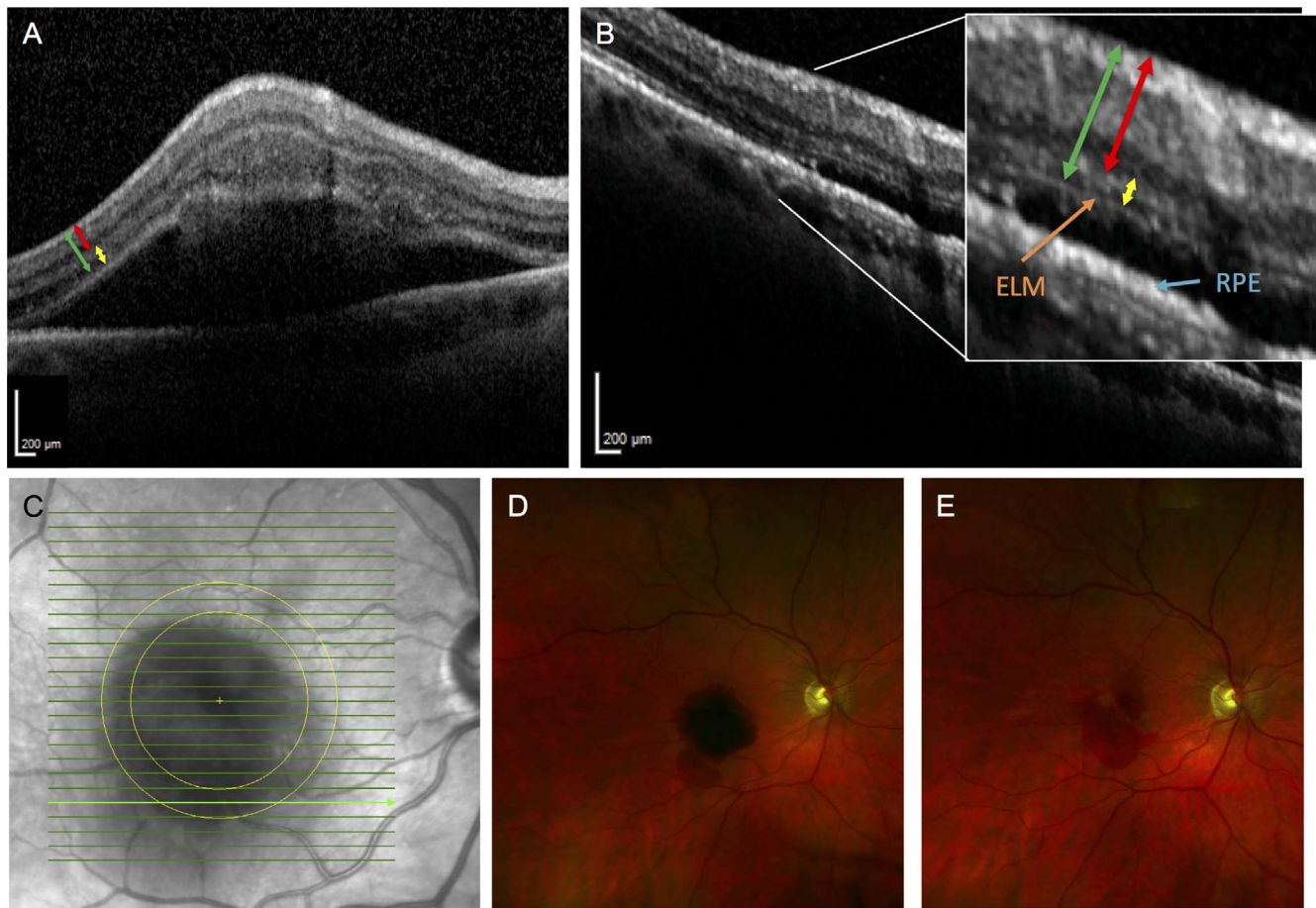


FIGURE 1. Fundus photographs and representative SD-OCT images of patient 3. (A) SD-OCT section of SMH involving the fovea prior to surgery shows a thickened inner and outer retina. The RPE is not visible underneath the SMH. The *red line* represents the measurement made for the IRT, the *yellow line* represents the ORT, and the *green line* represents the FRT. (B) Postoperative month 11.5 SD-OCT scan of the same area shows resolution of the SMH. The IRT and ORT appear qualitatively thinner. The ELM and RPE are also apparent now. The same color scheme in A is used to highlight the measurements for the retinal thicknesses. (C) Infrared fundus image of the retina with the *bold green line* representing the location of SD-OCT retinal thickness measurements before and after subretinal tPA displacement of SMH. (D) Preoperative fundus photograph shows the SMH covering the fovea. (E) Postoperative month 1 fundus photograph shows resolution of the SMH.

(AHK). No commercially available, automated measurements of the retina were used. The image contrast was manually set for each individual SD-OCT scan to optimize the signal-to-noise ratio and allow identification of relevant retinal anatomy, especially the retinal layers. Manual measurements were made to quantify the inner retinal thickness (IRT), outer retinal thickness (ORT), and full retinal thickness (FRT) in the 1:1- μm display, including those for oblique measurements. Although it was possible to identify the approximate location of outer retinal layers in subjects with SMH, the identification of the outer boundary of the ONL was at the discretion of the graders' best judgment and possibly prone to error. Therefore, we performed separate manual measurements of the IRT and ORT to remove any potential bias that would be introduced by manual measurements of the ORT. The IRT included the internal limiting membrane (ILM), retinal nerve fiber layer, ganglion cell layer, inner plexiform layer, and inner nuclear layer (INL). The ORT included the outer plexiform layer (OPL) and ONL. The border of the IRT and ORT at the junction between the INL and OPL was chosen, because this location was observed to be most clearly delineated across all pre- and postoperative SD-OCT scans (making the measurements most consistent and accurate for the IRT and ORT). The FRT spanned from the ILM to the outer boundary of the ONL.

Although a published nomenclature²⁴ outlined the retinal landmarks, and another previously published study²⁵ concluded that the automated Heidelberg Spectralis SD-OCT defines the full thickness retina to the outer boundary of the RPE, our dataset was limited by the variability in retinal anatomy and obscuration of the RPE, especially in preoperative SD-OCT scans of the retina overlying the SMH. To obtain consistent results across all scans, we avoided automated measurements and performed manual measurements in the areas overlying the SMH, corresponding normal areas in the untreated contralateral eye, and normal areas immediately adjacent to the SMH in the treated eye. However, measurements of the neurosensory retina spanning from the ILM to the inner boundary of the RPE were also performed in the normal, adjacent areas to detect changes in significant differences. In five pre- and one postoperative SD-OCT scans (Figs. 1A, 1B), the retina was oriented obliquely relative to the *x*-axis, so measurements were made perpendicular to the axis of the retina, rather than parallel to the green OCT line marker. The locations of the outer retinal landmarks were manually interpolated from adjacent normal regions in cases where the boundary of the outer layers was difficult to directly visualize due to the adjacent subretinal hemorrhage. This method has been previously described.²⁶ The visibility of the ELM, EZ, and RPE were also noted on each scan that was used for measurements.

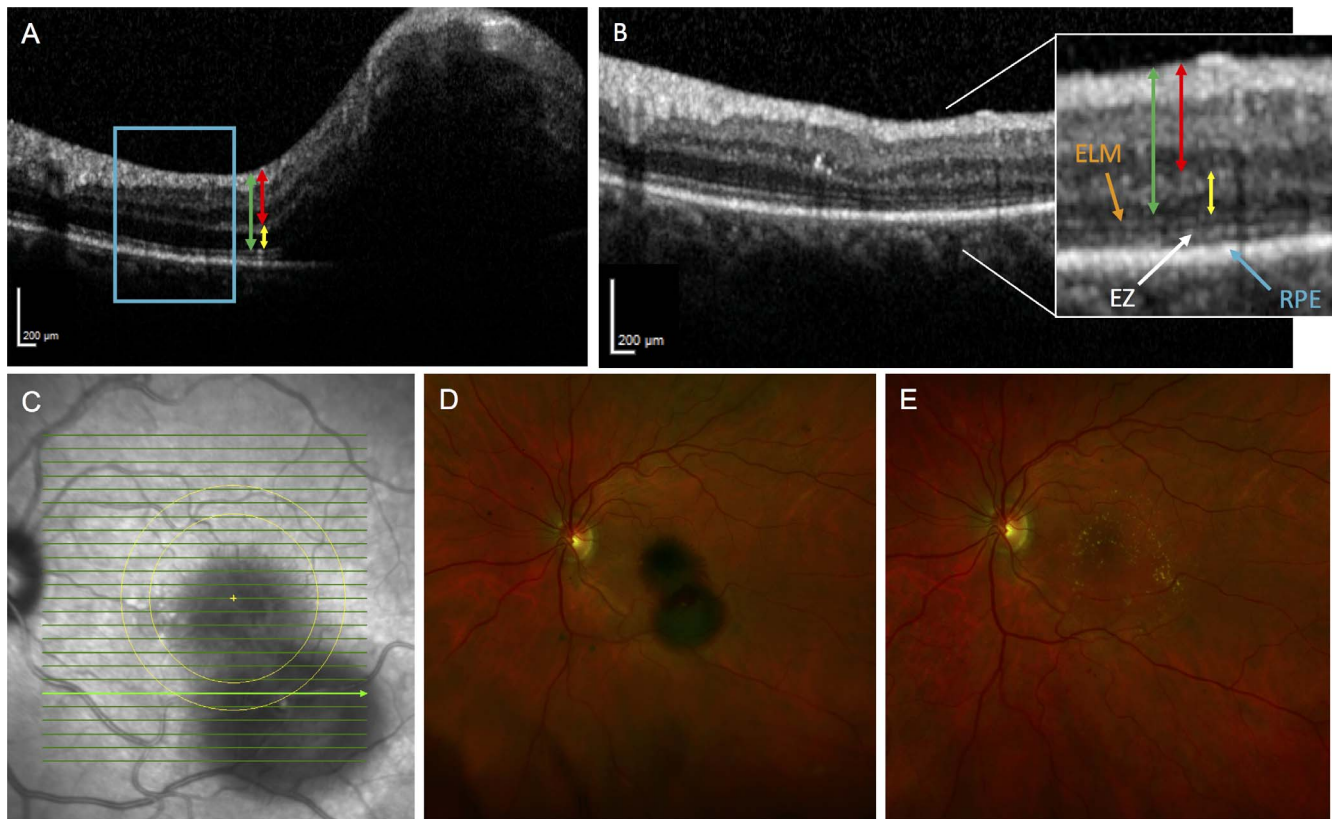


FIGURE 2. Fundus photographs and representative SD-OCT images of patient 6. (A) SD-OCT scan of a SMH involving the fovea prior to surgery shows thickened inner and outer retina. The ELM and EZ are not apparent in the area of the hemorrhage. The *blue rectangular region* adjacent to the hemorrhage highlights a normal area unaffected by the SMH but later detached by the induced RD. The *red line* represents the IRT, the *yellow line* represents the ORT, and the *green line* represents the FRT. (B) Postoperative month 11 SD-OCT scan of the same area captured in previous panel shows resolution of the SMH. The high-magnification image shows reappearance of the ELM and EZ. The same color scheme in A is used to highlight the measurements for the retinal thicknesses. (C) Infrared fundus image of macula with SD-OCT B-scan locations denoted in *green lines*. The two concentric *yellow circles* centered on the fovea with diameters of approximately 3 and 4 mm, respectively, are shown. The *bold green line* represents the location within the concentric circles where the SD-OCT-based retinal thickness measurements were made before and after the subretinal tPA displacement of SMH. (D) Preoperative fundus photograph showing the SMH. (E) Postoperative fundus photograph at month 2.5 of the nearly resolved SMH depicted in previous panel.

Retinal thickness measurements of the detached area overlying the SMH were obtained prior to surgery and repeated in the same areas following surgery. Many subjects did not have pre- or postoperative imaging sufficient for inclusion in this study. To perform standardized and reliable measurements, all measurements were obtained within a predefined circular annulus that had an approximate inner and outer diameter of 3 and 4 mm, respectively, and was centered on the fovea (Fig. 2). This predefined region of interest (ROI) was selected such that it would maximize the possibility of including both detached retina as well as normal retina within its boundaries across all cases. By performing retinal measurements in normal and abnormal areas within this ROI, the retinal thickness overlying areas of SMH could be compared with retinal thickness measurements from the contralateral eye but symmetrical locations of the macula that served as controls. In this way, the normal variations in retinal thickness due to retinal topology was not a confounding factor in the measurements.

In most cases, measurements of the retinal thicknesses were made at the 12 and 6 o'clock locations on the ROI for consistency and comparability between individual measurements on different dates and among subjects. If a normal region of attached retina was not observed within the prespecified ROI in the pathologic eye, similar corresponding measurements were made preoperatively in the contralateral unaffected eye to

serve as controls. Figure 3 is another schematic of preoperative and postoperative fundus photography illustrating the locations where retinal thickness measurements were made in the areas overlying the SMH and, if possible, in the normal unaffected locations immediately adjacent to the SMH. In addition, the retina highlighted in the blue box of Figure 2A is an example of a normal region that was unaffected by the SMH but affected by the induced focal, short-term retinal detachment. If normal areas were available for assessment on the OCT scans, qualitative assessments of the RPE, ELM, and EZ were also done in these areas.

Statistics

SPSS Statistics (IBM, Armonk, NY, USA) was used to perform the statistical analysis. Due to the small sample size and the non-normal distribution of data, nonparametric tests were performed. The Wilcoxon signed rank test was used to determine statistically significant differences in SD-OCT measurements and BCVA with a type I error less than 0.05.

RESULTS

Eleven patients with SMH and history of neovascular AMD were initially included in the study population. Seven eyes

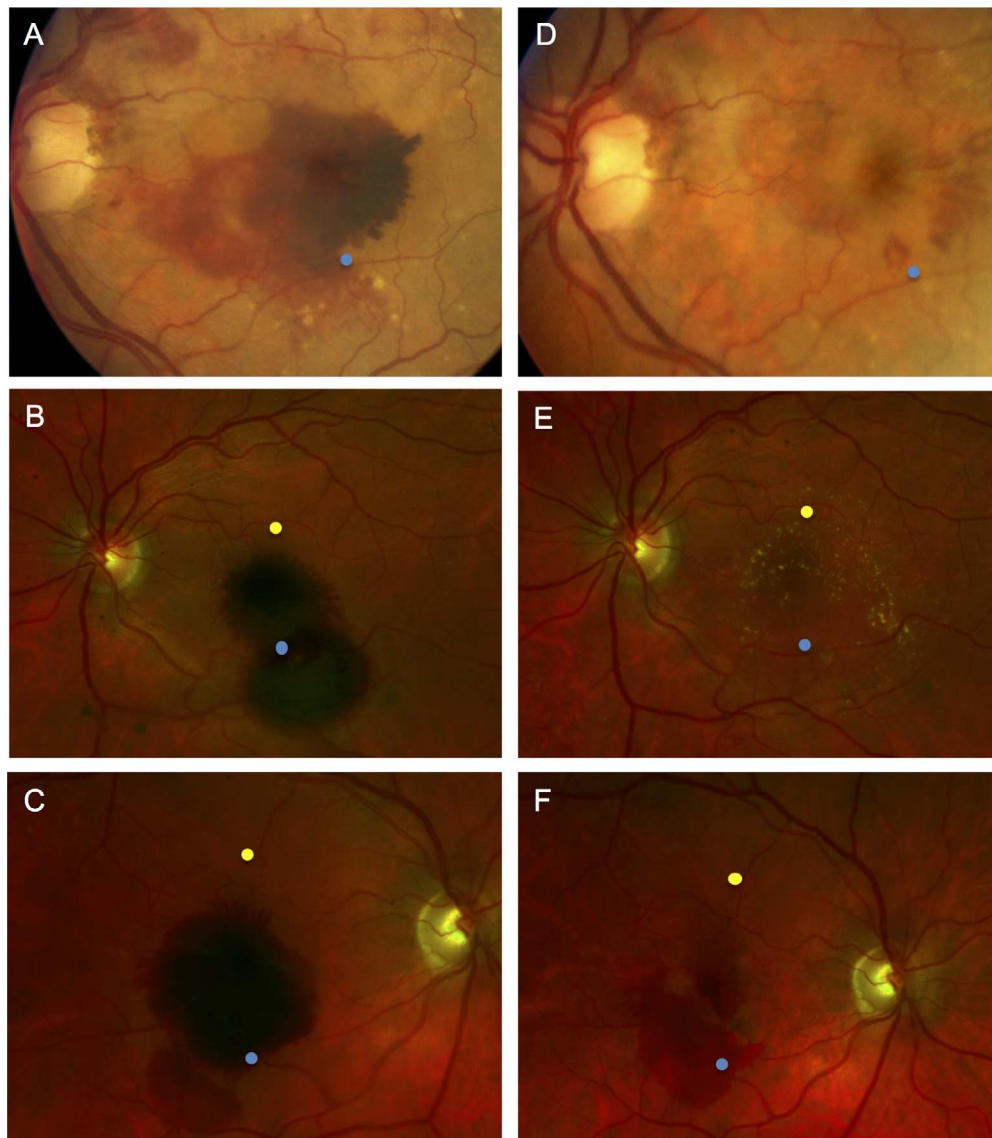


FIGURE 3. Schematic of the fundus locations where OCT measurement were made before and after subretinal tPA displacement of SMH. (A–C) Fundus photographs demonstrate large SMH. (D–F) Photographs demonstrate resolution of the hemorrhages following surgery and SMH displacement with subretinal tPA at 13, 11, and 1 months, respectively. The *blue points* represent the location of OCT retinal thickness measurements overlying the hemorrhage, and the *yellow points* represent the location of measurements made immediately adjacent to the hemorrhage (attached retina). Normal, attached retinal OCT sections were not available in regions immediately adjacent to the SMH for the eyes in A and D, so *yellow points* are not depicted.

from four patients were excluded due to inadequate SD-OCT scan quality and/or failure of the SMH to resolve by the end of the study period. Seven eyes from seven patients were included in the final analysis. Four eyes were included in the analysis for the normal attached areas, because the SMH was so large in other cases that normal retinal sections were not in the field of the SD-OCT scan. The final BCVA was significantly improved (0.81 ± 0.43 vs. 1.86 ± 0.70 logMAR; $P = 0.027$). The subject demographics are summarized in the Table.

Quantification of Retinal Thickness Adjacent to SMH

To examine the impact of surgically induced RD on the apparently normal retina surrounding the SMH, we performed retinal thickness measurements on four preoperative and four postoperative SD-OCT scans in completely attached retina

immediately adjacent (within 1 to 2 disc diameters or ~ 1.5 mm) to the SMH. These areas were all confirmed to be detached by visual inspection intraoperatively during the SMH displacement procedure by the surgeon. These measurements did not show changes in IRT (145 ± 19 vs. 149 ± 37 ; $P = 1.00$), ORT (87 ± 5 vs. 82 ± 8 μm ; $P = 0.11$), or FRT (292 ± 47 vs. 264 ± 34 μm ; $P = 0.47$) as a result of the RD induction (Fig. 4). To validate our results using more commonly accepted anatomical markers of ORT and FRT, we repeated the measurements of the ORT ($P = 0.11$) and the FRT ($P = 0.20$) to the inner boundary of the RPE. This analysis also showed no changes in thickness from before to after surgery.

Quantification of Retinal Thickness Overlying SMH

We performed measurements of the retinal thickness overlying the SMH for comparison with pre- and postoperative measure-

TABLE. Demographics and Clinical Characteristics of the Study Population

Patient	Age, y	Eye	Symptom Duration, days	Lens Status	Visual Acuity, logMAR*	IOP, mm Hg*	Retina Overlying SMH Visible*			Retina Surrounding SMH Visible*			Follow-up, mo
							ELM	EZ	RPE	ELM	EZ	RPE	
1	64	OS	6	Phakic	3.0	15	Yes	Yes	No	Yes	Yes	Yes	46
					0.9	16	Yes	Yes	Yes	Yes	Yes		
2	73	OD	29	PCIOL	1.9	15	No	No	Yes	Yes	Yes	Yes	11
					0.5	10	No	No	Yes	Yes	Yes		
3	68	OD	8	Phakic	1.9	14	No	No	Yes	Yes	Yes	Yes	20
					0.5	15	Yes	No	Yes	Yes	Yes		
4	80	OS	62	PCIOL	2.3	15	No	No	Yes	NA	NA	NA	18
					1.3	14	No	No	Yes	NA	NA		
5	79	OD	25	Phakic	1.9	7	No	Yes	Yes	NA	NA	NA	10
					1.3	13	No	No	Yes	NA	NA		
6	72	OS	12	PCIOL	1.0	13	No	No	No	Yes	Yes	Yes	15
					1.0	16	Yes	Yes	Yes	Yes	Yes		
7	72	OS	1	PCIOL	1.0	10	No	No	Yes	NA	NA	NA	9
					0.2	14	Yes	Yes	Yes	NA	NA		

SMH, submacular hemorrhage; IOP, intraocular pressure; ELM, external limiting membrane; EZ, ellipsoid zone; RPE, retinal pigment epithelium; NA, all areas available for analysis on OCT scans were affected by SMH, and no normal unaffected regions were visible.

* Values given represent the preoperative and postoperative condition with the preoperative value listed on top.

ments made in seven affected eyes and normal measurements made in the seven preoperative contralateral, unaffected eyes. Preoperative IRT, (222 ± 59 vs. 140 ± 17 μm ; $P=0.018$), ORT (203 ± 97 vs. 83 ± 12 μm ; $P=0.028$), and FRT (427 ± 63 vs. 264 ± 22 μm ; $P=0.018$) overlying the SMH were greater than corresponding normal areas in the contralateral unaffected eye (Fig. 5). The postoperative IRT in the areas overlying the SMH were greater compared with corresponding normal areas in the contralateral eye (171 ± 31 vs. 140 ± 17 μm ; $P=0.018$), but no differences were evident for the postoperative ORT (72 ± 34 vs. 83 ± 12 μm ; $P=0.31$) and FRT (289 ± 77 vs. 264 ± 22 μm ; $P=0.87$) compared with normal areas. The postoperative IRT (171 ± 31 vs. 222 ± 59 μm ; $P=0.028$), ORT (72 ± 34 vs. 203 ± 97 μm ; $P=0.043$), and FRT (289 ± 77 vs. 427 ± 63 μm ; $P=0.018$) overlying the SMH were decreased compared with preoperative thicknesses. Figures 1, 2, and 6 illustrate examples of pre- and postoperative fundus photos and SD-OCT scans with retinal thickness measurements shown.

Qualitative Assessment of Outer Retinal Banding Patterns

We assessed the impact of surgically induced RD on outer retinal structures in the normal region of retina surrounding the SMH that was incidentally detached during the SMH displacement procedure (Table). In all subjects in whom normal regions of retina immediately adjacent to the SMH were available to view on SD-OCT, the ELM, EZ, and RPE were visible and unchanged before and after surgery. This suggests that focal RD of these areas did not cause significant damage. In contrast, outer retinal structures overlying the SMH were more variably affected and less easily visible because of the overlying hemorrhage (Table).

DISCUSSION

Surgically induced RDs are becoming more commonplace in the delivery of gene and cell-based therapies. However, it is not known whether this form of RD has the same detrimental impact on retinal anatomy as pathologic retinal detachments such as RRD¹¹⁻¹⁵ or more chronically induced experimental

RD in animal models.^{4,7-9} The goal of this study is to determine whether a surgically induced focal RD of the normal retinal regions surrounding a SMH causes any detectable changes in retinal anatomy. This study was possible because patients with SMH often undergo PPV and a surgical displacement procedure, which incidentally detaches a small rim of normal retina around the SMH. This provides a unique opportunity to study the impact of this increasingly common procedure in the normal retina of human subjects.

This study is novel in that it uses a meticulous, manually guided protocol for measurement of retinal thickness in the unaffected (attached) retinal regions immediately surrounding the SMH. Specifically, we demonstrate that surgical induction of a focal, short-term RD to displace a SMH does not cause significant changes in retinal thickness, as detected by SD-OCT, in regions of the attached retina that are incidentally detached by this surgical procedure.

Our study also confirms previous SD-OCT-based findings of thickness changes in the retinal regions overlying the SMH that have been demonstrated by other investigators.¹⁷ This validates the methods that we used to make our observations. Although the mean ORT was greater overlying the SMH, this measurement had a large SD because it was difficult to reliably identify the outer retinal boundaries in the presence of SMH in at least some cases. We performed manual measurements of the IRT, in addition to the ORT and FRT, to remove any potential bias that would be introduced by relying on the sometimes poorly apparent outer boundaries of the ORT and FRT for accurate measurements. The IRT was less prone to bias, since its boundaries were always clearly identifiable. The mean IRT and FRT overlying the SMH prior to surgery were both significantly greater than topographically similar normal regions in the normal contralateral eye (Fig. 5). This increase in thickness is likely due to microscopic intraretinal edema that has been demonstrated in animal and human studies.⁵ Measurements in the normal contralateral eye were only performed preoperatively and not repeated postoperatively for comparison to measurements in the postoperative affected eye. Lack of repeat postoperative measurements in the normal contralateral eye likely does not affect the results, because a previous study indicated no significant changes in diurnal variations in SD-OCT.²⁷

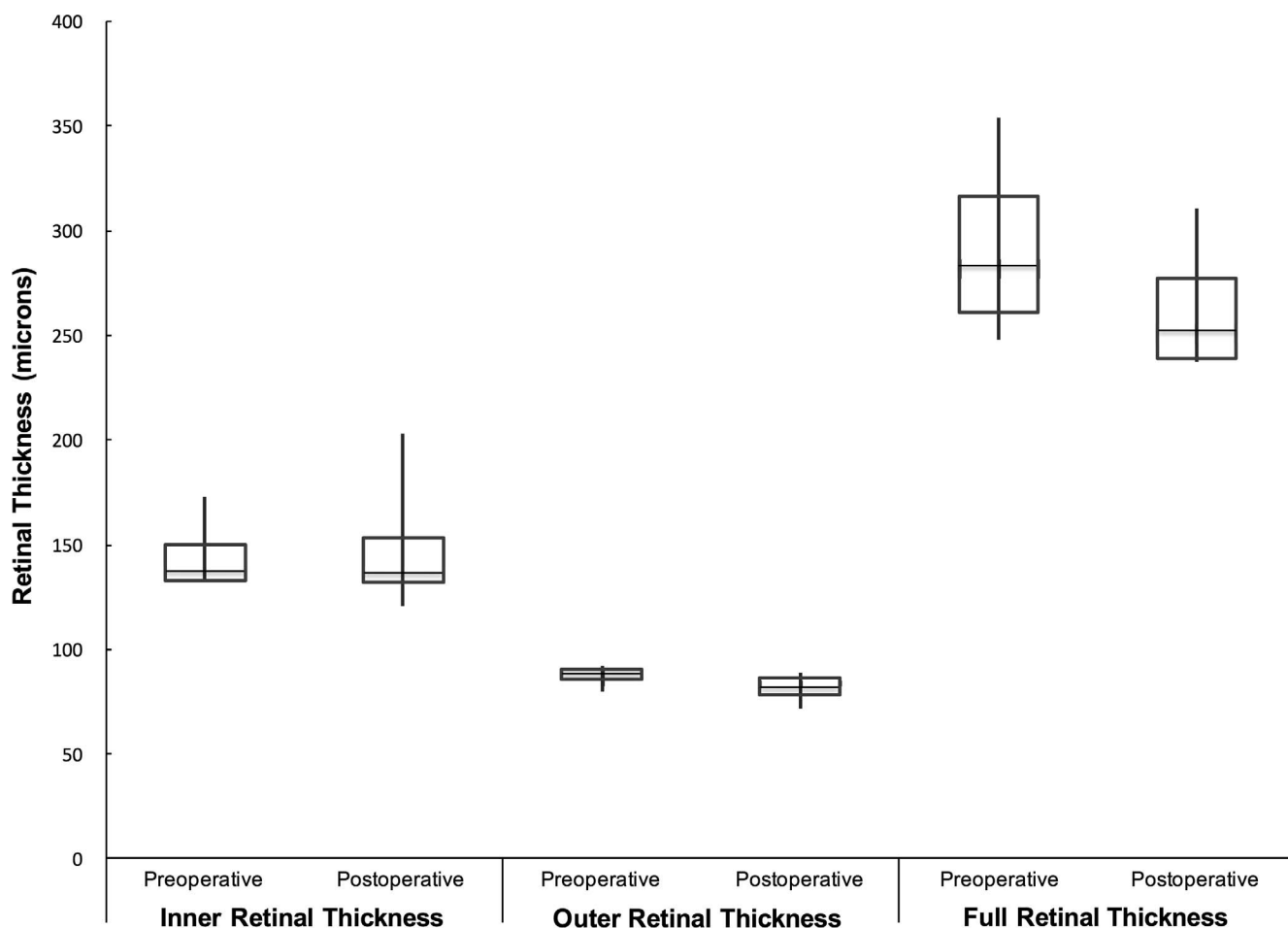


FIGURE 4. This box-and-whisker plot illustrates the inner, outer, and full retinal thicknesses of the attached retinal areas immediately adjacent to the SMH before and after the subretinal tPA injection and induced retinal detachment. The retinal thicknesses of these normal areas did not significantly change for either the inner, outer, or full retinal thicknesses as a result of the induced RD.

Despite our understanding of the retinal landmarks,²⁴ not all of the preoperative SD-OCT scans had an easily identifiable RPE so we chose to use the outer border of the ONL as the outer border of the ORT and FRT. To standardize measurements across all SD-OCT scans, we used the same segmentation scheme, even in scans that included an identifiable RPE. Although this method is imperfect, it was the most reliable method to standardize measurements, and our findings in the regions overlying the SMH are supported by previous findings using SD-OCT-based methods to evaluate retinal thickness changes following SMH.¹⁷ However, to evaluate the difference in statistical significance based on segmentation scheme, we performed measurements of the ORT and FRT to the inner boundary of the RPE in the normal areas adjacent to the SMH affected by the induced RD but with normal retinal landmarks. Even in these repeat measurements, the ORT and FRT were not different from before to after surgery, suggesting that segmentation scheme does not bias the overall significance of our findings.

Our manual measurements were oriented perpendicular to the retinal surface to accurately measure the retinal thicknesses, especially in the preoperative SD-OCT scans. In the 1:1- μ m display of the Heidelberg OCT images, obliquely oriented measurements accurately measure the retinal thicknesses, based on a previous study that indicated measurements oriented perpendicular to the retina in the 1:1- μ m display are more accurate, especially in obliquely oriented images.²⁸ This

was confirmed with oblique measurements made in relation to the 200- μ m scale observed in the scans. If the measurements were oriented parallel to the green OCT line marker, the measurements would not accurately reflect the retinal thicknesses, leading to inconclusive results.

Postoperative ORT and FRT after SMH displacement were not significantly different from topographically similar normal retinal regions (Fig. 5), presumably due to the resolution of microscopic intraretinal edema, although this may also represent a loss of photoreceptors.²⁹ In agreement with most other studies, these findings demonstrate that surgical displacement of SMH can improve vision^{16,19} and at least restore retinal anatomy with minimal apparent damage to the areas involved in the SMH.^{17,20,21} Nevertheless, the effectiveness of surgical displacement is somewhat controversial, because there are reports of spontaneous visual improvement without any intervention,³⁰ as well as lack of improvement in at least some cases.¹⁹

Our findings suggest that the results of studies showing anatomic changes after pathologic RRD may not apply to surgically induced focal RD in humans. Similarly, the sometimes dramatic changes in retinal anatomy that have been described in experimental models of chronic RD³¹ also should be interpreted with caution when applied to human subjects. We hypothesize that this difference is because both pathologic RRD and more chronic, experimental RD in animal models last several days or more, whereas the surgically induced focal RD

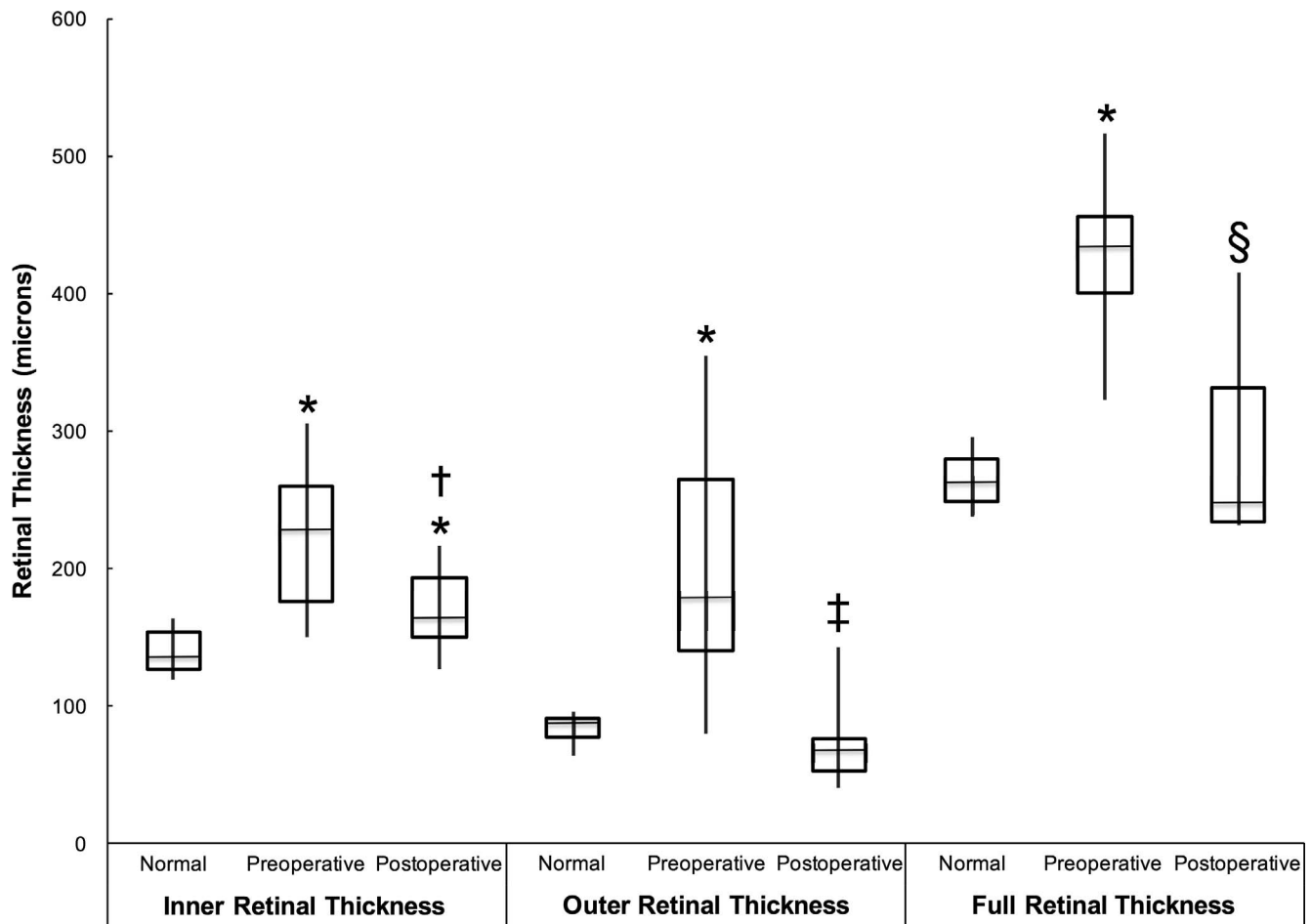


FIGURE 5. This box-and-whisker plot illustrates the changes in retinal thicknesses for the inner, outer, and full retinal thicknesses overlying the SMH before and after surgery. Retinal measurements in the normal, contralateral eye are also provided for comparison and control. The significance of individual comparisons is shown by the symbols: *significant difference with $P < 0.028$ compared with the respective normal measurement; †significant difference with $P < 0.028$ compared with the IRT before surgery; ‡significant difference with $P < 0.043$ compared with the ORT before surgery; §significant difference with $P < 0.018$ compared with the FRT before surgery.

lasts less than 1 day and likely less than several hours. In no case did the authors observe the persistence of a surgically induced RD on the first postoperative day. In addition, there may be other less controlled factors that mitigate against retinal damage in surgically induced RD, such as continuous intraocular irrigation (which would remove inflammatory mediators) and standard use of preoperative and postoperative steroids.

There has also been evidence to suggest that transient iatrogenic subfoveal injections may cause damage to the foveal cones, resulting in foveal thinning. Six of the eyes affected by SMH in our study had hemorrhages underlying the fovea, so the transient surgically induced RD affected the fovea as well. Jacobson et al.³² assessed the efficacy of subfoveal gene therapy injections for the treatment of Leber congenital amaurosis in a phase I study. Their analysis of pre- and postoperative SD-OCT scans indicated that two of five patients with a foveal detachment had significant long-term thinning of the fovea, accounting for intervisit variability, and the other three patients had either no long-term change in foveal thinning or insignificant foveal thinning. In addition, foveal thinning was noted in a patient without a foveal injection and the untreated eye of another patient.³² These findings suggest that the long-term foveal thinning may be related to the natural disease course, rather than the subfoveal injections. At 30 days

postoperatively, the short-term disruption in photoreceptor inner and outer segments may be related to the subfoveal injections, but these changes were noted to be recovered with longer follow-up,³² suggesting that subfoveal detachment is not related to permanent damage to the retina. Our study included patients that had a longer follow-up period ranging from 9 to 46 months, and our long-term results are consistent with the long-term findings of Jacobson et al.³² Resolution of the retinal anatomy over a long period was required for accurate measurements of retinal thicknesses on SD-OCT scans, so collection of short-term changes in retinal thickness likely would have resulted in unreliable results.

The limitations of our study include potential bias of manual measurements, small sample size, the retrospective nature of the study, and lack of confirmation of the incidental detachment of the adjacent, normal retina with intraoperative SD-OCT. A similar controlled or prospective study would be difficult to organize, because it would require a multicenter study over a prolonged period, given the relatively low frequency of large SMH undergoing surgical displacement. Our sample size was also small due to exclusion criteria that eliminated patients who did not have high-quality SD-OCT scans of both normal and pathologic areas for comparison. Because of the small sample size, the power of the study was inadequate in detecting small statistically significant differences.

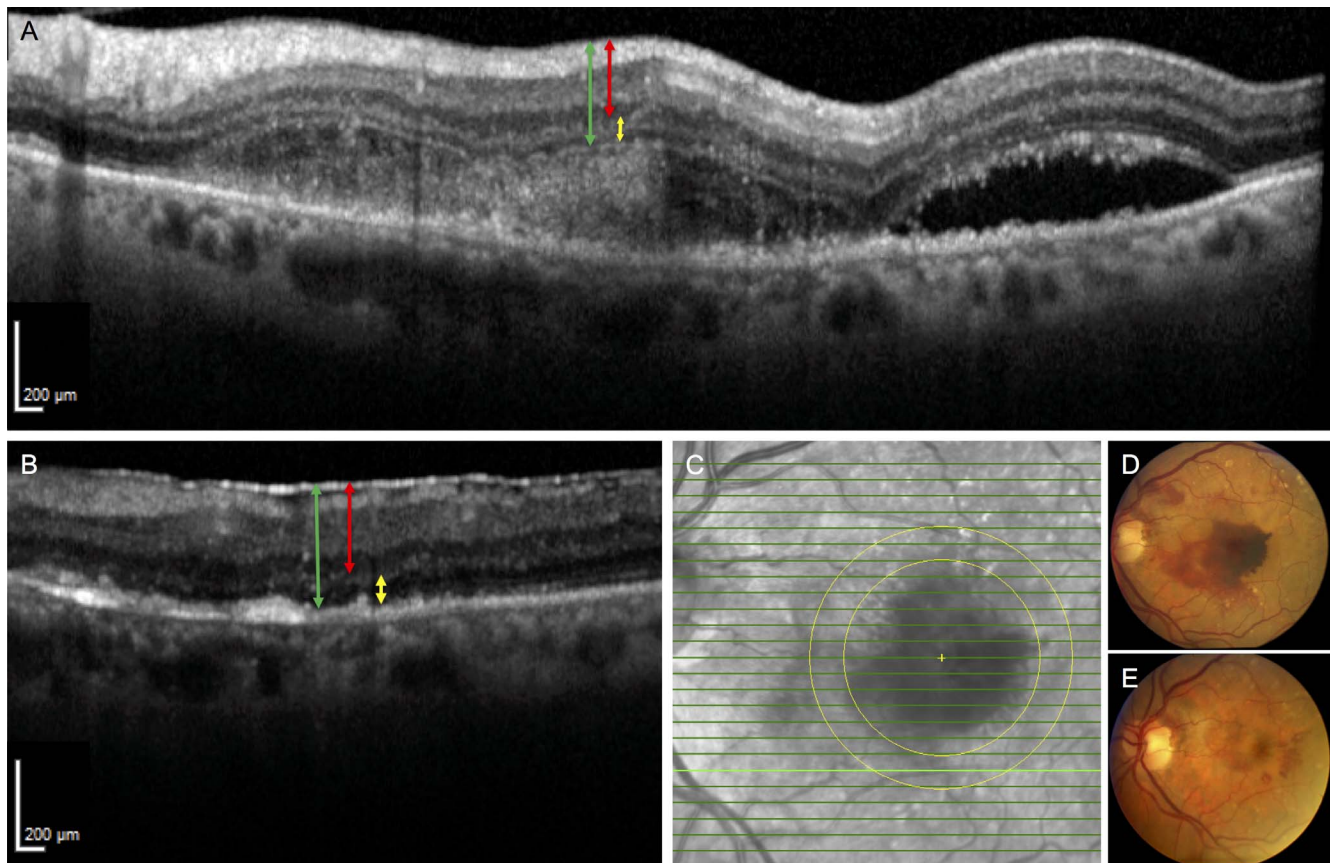


FIGURE 6. Fundus photographs and representative SD-OCT images of patient 4. (A) Wide-field, high-magnification SD-OCT of SMH involving the fovea prior to surgery shows thickened inner and outer retina. (B) Postoperative month 13 SD-OCT scan of the same area captured in previous panel after subretinal tPA displacement. The *red line* represents the measurement made for the IRT, the *yellow line* represents the ORT, and the *green line* represents the FRT. (C) Infrared fundus image of the macula with the bolded green line representing the location within the concentric circles where the measurements were made before and after subretinal tPA displacement of SMH. (D) Preoperative fundus photograph showing the SMH. (E) Postoperative month 3 fundus photograph of the nearly resolved SMH in previous panel.

es. We attempted to mitigate these limitations by performing separate measurements of the IRT and ORT to minimize potential error from distortion of outer retinal features secondary to the SMH. In addition, we developed a very careful measurement protocol to compare topographically similar regions of the retina that could serve as internal controls.

Another limitation of our study involves the inability of SD-OCT to detect ultrastructural changes to the retina and underlying RPE. Histologic studies in animal models have demonstrated subtle changes in retinal anatomy that are likely below the limit of detection of SD-OCT.⁷ For example, Szurman et al.⁶ noted subcellular changes in retina and RPE on electron microscopy that are likely not detectable on SD-OCT. It is interesting, however, that we were able to detect a small, significant increase in postoperative IRT compared with the normal, contralateral eye, even after SMH displacement (Fig. 5). This may represent the macroscopic result of otherwise undetectable interstitial and intracellular edema throughout the whole retina. Nevertheless, we cannot rule out that surgically induced focal RD causes minor ultrastructural changes that cannot be detected on SD-OCT as demonstrated in histologic studies of transient retinal detachments.³³ However, studies also indicated long-term damage to photoreceptors can be stopped, possibly even reversed,³⁴ by rapid reattachment, preferably less than 1 day.³³ Our results suggest even if minor damage is induced, it is not severe enough to cause changes in SD-OCT. Because surgical induction of focal

RD is only performed in cases of relatively severe vision loss, the overall benefits of the therapeutic procedure may outweigh any potentially undetectable retinal damage from the induced detachment procedure. Histologic studies in humans following surgical detachment of the retina is not feasible, and these data are still clinically relevant and important, especially for therapies requiring access to the subretinal space.

In conclusion, our results show that surgical induction of a short-term, focal retinal detachment does not cause changes in retinal anatomy that can be detected by SD-OCT. This finding supports the growing use of this procedure in the delivery of gene and cell-based therapies to the retina in subjects with severe vision loss.

Acknowledgments

Supported by National Institutes of Health Grant K08EY027006 and an unrestricted grant from Research to Prevent Blindness (New York, NY, USA).

Disclosure: **K. Kogachi**, None; **J.D. Wolfe**, None; **A.H. Kashani**, Carl Zeiss Meditec (F, R)

References

1. MacLaren RE, Groppe M, Barnard AR, et al. Retinal gene therapy in patients with choroideremia: initial findings from a phase 1/2 clinical trial. *Lancet*. 2014;383:1129–1137.

2. Schwartz SD, Regillo CD, Lam BL, et al. Human embryonic stem cell-derived retinal pigment epithelium in patients with age-related macular degeneration and Stargardt's macular dystrophy: follow-up of two open-label phase 1/2 studies. *Lancet*. 2015;385:509-516.
3. Murakami Y, Notomi S, Hisatomi T, et al. Photoreceptor cell death and rescue in retinal detachment and degenerations. *Prog Retin Eye Res*. 2013;37:114-140.
4. Faude F, Francke M, Makarov F, et al. Experimental retinal detachment causes widespread and multilayered degeneration in rabbit retina. *J Neurocytol*. 2001;30:379-390.
5. Faude F, Wendt S, Biedermann B, et al. Facilitation of artificial retinal detachment for macular translocation surgery tested in rabbit. *Invest Ophthalmol Vis Sci*. 2001;42:1328-1337.
6. Szurman P, Roters S, Grisanti S, et al. Ultrastructural changes after artificial retinal detachment with modified retinal adhesion. *Invest Ophthalmol Vis Sci*. 2006;47:4983-4989.
7. Yang L, Kim JH, Kovacs KD, Arroyo JG, Chen DF. Minocycline inhibition of photoreceptor degeneration. *Arch Ophthalmol*. 2009;127:1475-1480.
8. Cook B, Lewis GP, Fisher SK, Adler R. Apoptotic photoreceptor degeneration in experimental retinal detachment. *Invest Ophthalmol Vis Sci*. 1995;36:990-996.
9. Hisatomi T, Sakamoto T, Goto Y, et al. Critical role of photoreceptor apoptosis in functional damage after retinal detachment. *Curr Eye Res*. 2002;24:161-172.
10. Arroyo JG, Yang L, Bula D, Chen DF. Photoreceptor apoptosis in human retinal detachment. *Am J Ophthalmol*. 2005;139:605-610.
11. Gharbiya M, Grandinetti F, Scavella V, et al. Correlation between spectral-domain optical coherence tomography findings and visual outcome after primary rhegmatogenous retinal detachment repair. *Retina*. 2012;32:43-53.
12. Schocket LS, Witkin AJ, Fujimoto JG, et al. Ultrahigh-resolution optical coherence tomography in patients with decreased visual acuity after retinal detachment repair. *Ophthalmology*. 2006;113:666-672.
13. dell'Omo R, Viggiano D, Giorgio D, et al. Restoration of foveal thickness and architecture after macula-off retinal detachment repair. *Invest Ophthalmol Vis Sci*. 2015;56:1040-1050.
14. Mandai M, Watanabe A, Kurimoto Y, et al. Autologous induced stem-cell-derived retinal cells for macular degeneration. *N Engl J Med*. 2017;376:1038-1046.
15. Shirai H, Mandai M, Matsushita K, et al. Transplantation of human embryonic stem cell-derived retinal tissue in two primate models of retinal degeneration. *Proc Natl Acad Sci U S A*. 2016;113:E81-E90.
16. Chang W, Garg SJ, Maturi R, et al. Management of thick submacular hemorrhage with subretinal tissue plasminogen activator and pneumatic displacement for age-related macular degeneration. *Am J Ophthalmol*. 2014;157:1250-1257.
17. Kadonosono K, Arakawa A, Yamane S, et al. Displacement of submacular hemorrhages in age-related macular degeneration with subretinal tissue plasminogen activator and air. *Ophthalmology*. 2015;122:123-128.
18. Hillenkamp J, Surguch V, Framme C, Gabel VP, Sachs HG. Management of submacular hemorrhage with intravitreal versus subretinal injection of recombinant tissue plasminogen activator. *Graefes Arch Clin Exp Ophthalmol*. 2010;248:5-11.
19. Hauptert CL, McCuen BW, Jaffe GJ, et al. Pars plana vitrectomy, subretinal injection of tissue plasminogen activator, and fluid-gas exchange for displacement of thick submacular hemorrhage in age-related macular degeneration. *Am J Ophthalmol*. 2001;131:208-215.
20. Kimura S, Morizane Y, Hosokawa M, et al. Submacular hemorrhage in polypoidal choroidal vasculopathy treated by vitrectomy and subretinal tissue plasminogen activator. *Am J Ophthalmol*. 2015;159:683-689.
21. Inoue M, Shiraga F, Shirakata Y, Morizane Y, Kimura S, Hirakata A. Subretinal injection of recombinant tissue plasminogen activator for submacular hemorrhage associated with ruptured retinal arterial macroaneurysm. *Graefes Arch Clin Exp Ophthalmol*. 2015;253:1663-1669.
22. Olivier S, Chow DR, Packo KH, MacCumber MW, Awh CC. Subretinal recombinant tissue plasminogen activator injection and pneumatic displacement of thick submacular hemorrhage in age-related macular degeneration. *Ophthalmology*. 2004;111:1201-1208.
23. Schulze-Bonsel K, Feltgen N, Burau H, Hansen L, Bach M. Visual acuities "hand motion" and "counting fingers" can be quantified with the freiburg visual acuity test. *Invest Ophthalmol Vis Sci*. 2006;47:1236-1240.
24. Staurengi G, Sadda S, Chakravarthy U, Spaide RF. Panel INFOCTIO. Proposed lexicon for anatomic landmarks in normal posterior segment spectral-domain optical coherence tomography: the IN•OCT consensus. *Ophthalmology*. 2014;121:1572-1578.
25. Wolf-Schnurrbusch UE, Ceklic L, Brinkmann CK, et al. Macular thickness measurements in healthy eyes using six different optical coherence tomography instruments. *Invest Ophthalmol Vis Sci*. 2009;50:3432-3437.
26. Kashani AH, Keane PA, Dustin L, Walsh AC, Sadda SR. Quantitative subanalysis of cystoid spaces and outer nuclear layer using optical coherence tomography in age-related macular degeneration. *Invest Ophthalmol Vis Sci*. 2009;50:3366-3373.
27. Jo YJ, Heo DW, Shin YI, Kim JY. Diurnal variation of retina thickness measured with time domain and spectral domain optical coherence tomography in healthy subjects. *Invest Ophthalmol Vis Sci*. 2011;52:6497-6500.
28. Kim JH, Kang SW, Ha HS, Kim SJ, Kim JR. Overestimation of subfoveal choroidal thickness by measurement based on horizontally compressed optical coherence tomography images. *Graefes Arch Clin Exp Ophthalmol*. 2013;251:1091-1096.
29. Glatt H, Macherer R. Experimental subretinal hemorrhage in rabbits. *Am J Ophthalmol*. 1982;94:762-773.
30. Chaudhry NA, Flynn HW, Lewis ML. Spontaneous resolution of submacular hemorrhage with marked visual improvement. *Ophthalmic Surg Lasers*. 1999;30:670-671.
31. Bartuma H, Petrus-Reurer S, Aronsson M, Westman S, André H, Kvanta A. In vivo imaging of subretinal bleb-induced outer retinal degeneration in the rabbit. *Invest Ophthalmol Vis Sci*. 2015;56:2423-2430.
32. Jacobson SG, Cideciyan AV, Ratnakaram R, et al. Gene therapy for leber congenital amaurosis caused by RPE65 mutations: safety and efficacy in 15 children and adults followed up to 3 years. *Arch Ophthalmol*. 2012;130:9-24.
33. Lewis GP, Charteris DG, Sethi CS, Leitner WP, Linberg KA, Fisher SK. The ability of rapid retinal reattachment to stop or reverse the cellular and molecular events initiated by detachment. *Invest Ophthalmol Vis Sci*. 2002;43:2412-2420.
34. Guerin CJ, Lewis GP, Fisher SK, Anderson DH. Recovery of photoreceptor outer segment length and analysis of membrane assembly rates in regenerating primate photoreceptor outer segments. *Invest Ophthalmol Vis Sci*. 1993;34:175-183.